IEEE Access
Multidisciplinary | Rapid Review | Open Access Journal

Received March 25, 2020, accepted April 21, 2020, date of publication May 11, 2020, date of current version May 22, 2020.

Digital Object Identifier 10.1109/ACCESS.2020.2993576

Device-Free Localization Scheme With Time-Varying Gestures Using Block Compressive Sensing

YAN GUO, SIXING YANG, NING LI, AND XINHUA JIANG
College of Communications Engineering, Army Engineering University, Nanjing 210007, China
Corresponding author: Sixing Yang (guoyan_1029@sina.com)

This work was supported in part by the National Natural Science Foundation of China under Grant 61871400, and in part by the Natural Science Foundation of Jiangsu Province under Grant BK20171401.

ABSTRACT In Device-Free Localization (DFL) schemes, most researches assume that the targets are stationary with fixed gestures and motions. However, objects always change their gestures in practice, undoubtedly influencing the localization accuracy. To solve the issue, we propose a new algorithm named Ges-DFL under the Compressive Sensing (CS) framework, which considers the time-varying target gestures in the DFL scheme. Firstly, leaning that the matrixes referring to different target gestures cannot be achieved, we transfer them to a fixed sensing matrix by the transferring method. Secondly, we build the localization scheme as an MMV recovery issue and exploit the block sparsity property of transferred location vectors to improve the localization accuracy. Thirdly, the new algorithm Ges-DFL scheme is designed under the framework of the variational Bayesian inference to reconstruct transferred location vectors. Simulations show that the proposed algorithm performs well both in localization accuracy and robustness.

INDEX TERMS Multi-target localization, device free localization, compressive sensing, variational EM algorithm, block sparsity.

I. INTRODUCTION

Wireless Sensor Networks (WSN) [1], [2] have been widely deployed in our daily lives, significantly improving the quality of life. As one of the essential techniques in WSN, target localization has caught a lot of interest. The device-based localization scheme requires that the target is capable of producing and transmitting signals, which has been the most popular localization scheme [3]. However, targets cannot be equipped with devices to send signals in some cases, in which the device-based localization scheme is invalid [4]. For example, in smart homes, we would like to detect the station of the elderly and the kids, but the devices may affect their daily activities and may be lost by the kids, making the localization assignment interrupted [5]. In the defense field, the hostile equipment and army would not send us helpful localization information actively [6]. In the social security domain, the intruder makes great efforts to escape from being detected, undoubtedly not providing the helpful localization signal [7]. Coming to this, the Device-Free Localization (DFL) scheme, requiring no devices to be attached to targets, is becoming more and more popular [8].

DFL scheme is firstly proposed in work [9], where Yourself *et al.* build the DFL scene. It states that once the targets enter into the detecting area, they will predictively influence the wireless signal, rendering a relationship between the changed signal and the target position. Following the idea, several couples of transceivers and receivers, constituting the wireless links, are deployed to achieve the changed signals caused by targets [10]. Generally, a large number of wireless links are commanded to ensure localization accuracy. However, devices are always battery-powered. More wireless links will undoubtedly result in more energy costs, more extensive networks, and broader communication bands, much limiting the development of the DFL scheme [11].

Compressive Sensing (CS) [12] can reconstruct the sparse signal with much fewer samplings compared with the traditional Nyquist sampling theory, introducing a novel idea for the DFL scheme. In paper [13], Wang applied this theory in DFL, significantly reducing the required wireless links

The associate editor coordinating the review of this manuscript and approving it for publication was Qingchun Chen.

as well as guaranteeing the localization performance. Then many types of researches are involved in the CS-based DFL scheme. The work in paper [14] exploits the dictionary refinement issue, which can well solve the multiple target localization issue. Paper [15] proposes a dictionary building approach that can build the dictionary in the new field using only a few samplings, which saves much human effort involved in building the dictionary. Paper [11] considers the energy efficiency issue and proposes a quantized scheme in DFL, which can guarantee the target localization only by a few bits. Moreover, many papers exploit the target gesture identification, which highlights the influence of target gestures in DFL. Paper [16] propose an algorithm named WiFall, which can detect the fall of the older people in smart house. And some papers investigate the target gestures, which requires more accurate information when compared with the target localization scheme [17], [18].

However, seldom of the existing researches take considerations of the different target gestures and motions in DFL, and targets are always defaulted to be at fixed station. In other words, the dictionary is built under the fixed station of the targets, and then the target is assumed to be with the same gestures all the time [19]. Undoubtedly, this type of assumption will be invalid in practice. As we all know, some targets, like human beings, animals, may change their gestures all the time even when they are at a fixed location, undoubtedly can influence the wireless signal differently. For the other kind of category, like cars, tables, their different directions can also change the wireless signal accordingly. All in all, targets are always moving and will not be on the stationary way, making the assumption that targets are with fixed gestures less effective. Coming to this, we find it imperative to consider the target gestures in DFL.

Some issues should be noticed when solving the question. On the one hand, target with different gestures may affect the wireless signal uniquely, and building all types of dictionaries to suit the target gestures may be a massive waste of human effort. On the other hand, the target gestures can not be known ahead of time, making it impossible to select an applicable dictionary to avoid the dictionary mismatch. Thus we propose a novel CS-based DFL scheme named Ges-DFL. The new algorithm do not require to build all types of dictionaries under the different gestures, and only one dictionary is enough to achieve the target position. The contribution of the algorithm is as follows:

- We consider the influence of the target gestures and motions in DFL scheme for the first time, which can greatly improves the localization accuracy.
- Realizing that the dictionary according to different target gestures and motions can not be obtained, we apply the transferring method to guarantee the localization performance only by one dictionary.
- We build the DFL scheme as a novel Multiple Measurement Vectors (MMV) recovery issue and apply the block sparse vector recovery concept to exploit the relationship of the transferred location vectors.
- A new algorithm named Ges-DFL is proposed to recovery the lotion vectors under the variational Bayesian inference framework, which takes significant consideration of the correlation among the location vectors.

The rest of the passage is organized as follows: Section II introduces the related works. Section III describes the designed block sparsity DFL scheme, and the newly Ges-DFL recovery algorithm is shown in section IV. Then the performance of the proposed scheme is tested in Section V and section VI gives the conclusion of this research.

II. RELATED WORK

A. THE DFL THEORY

Several types of signals can be as the localization information to achieve the target positions in the DFL scheme. The image signal is the most popular signal applied in visual localization and tracking [20], [21]. However, the massage can be dramatically interrupted in the smog, dark and covered scene, as well as raising the risk of privacy disclosure. The infrared signal is applied under the condition that the devices can transmit and receive the infrared signals, requiring extra devices [22]. Paper [23] exploits the Channel Station Information (CSI) in DFL, which is more robust and can provide more localization information to guarantee the localization accuracy. However, this type of signal requires the wireless links to be under the framework of Orthogonal Frequency Division Multiplexing (OFDM), limiting the extensive application. Received Signal Strength (RSS) signal, easily to be obtained by almost all the devices and performs well even in the adverse scene, is the most suitable signal in the DFL scheme.

As we know, targets inside the detecting area of wireless links may reflect, shelf, and absorb the wireless signal, undoubtedly leading to the RSS changes. The wireless links are employed to collect the information. They are made up of pairs of transceivers and receivers, where the receivers can measure the RSS values transmitted from transceivers. And then, the signal changes can be calculated by comparing the RSS values of target outside and inside the affected area of wireless links.

The two main ways to achieve the RSS changes are the experiment-based [24] and model-based methods, respectively. The experiment-based approach builds the dictionary by testing. All the wireless links are ordered to measure the signal changes while fixing the target move through the whole grid points one by one, which can extremely approximate the environment. However, the sensing dictionary is required to be updated when coming to a new scene, abusing a large number of human effort. Model-based methods are set to approximate the signal changes caused by target entering into the location area using the model, which can save the human effort. Many existing types of researches involve in the DFL model designing. The binary model in paper [25] can provide rough information that weather the target is inside the effected domain of wireless link or not. Paper [26] approximates the affected area of a wireless link as an ellipse, which includes the distance information between the target

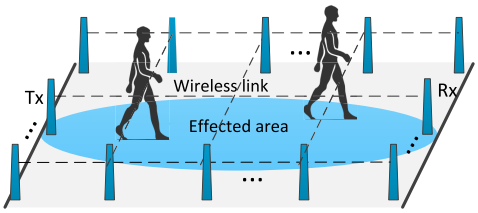

FIGURE 1. The illustration of the CS-based DFL scheme.

and the wireless links. Saddle Surface model can accurately describe the signal value caused by the target at different lotions, which can also provide distance information between the target and the transceivers/receivers when compared with the ellipse model [27]. Thus, we apply the Saddle Model in our DFL scheme to approximate the localization information.

B. THE CS-BASED DFL SCHEME

The CS-based DFL scheme demands fewer measurements to guarantee the reconstruction efficiency when compared with the traditional one. For that CS theory operates the discrete data, the localization area is divided into N grids as Figure1. K ($K \ll N$) targets are randomly at the grid points, whose positions can be represented as a N dimensions sparse signal. To collect RSS changes caused by targets, M ($M \ll N$) wireless links are deployed around the location area. Then the sensing equation could be obtained as follows:

$$y = Aw + n. \tag{1}$$

Location vector w**:** it is s a K sparse vector with N dimensions. Once $w_i = 1$, there is one target locating at the grid point i; otherwise, there are no targets. Note that the grid number N is always large enough, making it reasonable that targets are assumed to be exactly at the grid points.

Sensing matrix A**:** it represents the signal changes caused by the targets at different grid points, in which the element A_{mn} represents the signal changes of wireless link m influenced by target located at grid point n.

Measurement vector y**:** it represents the measurements of the wireless links caused by all the target located at the detecting area.

Measurement noise n**:** it is applied to approximate the noise.

Note that the measurement caused by multiple targets is not the direct accumulation of the signal changes caused by the single target, for that multiple targets may affect the same wireless link. However, the affected area of the wireless link is always limited and the target always independent with each other, making the probability that different targets being located at the detecting area of the same wireless link low. Following the most popular researches [13], [14], [28], we operate the target as independent options and assume that they do not affect the same wireless links.

III. THE GES-DFL MODEL

In the DFL scheme, targets do not change their coordinates suddenly, so we can collect the samplings in a short time slots with the same target positions. However, targets are not stationary. Kids, older adults, and pets are all possible to appear, and they may jump, sit down, stand on, fall, and so on, inevitably leading to different signal changes. The relating equations with L measurements are as follows:

$$\left[y^{(1)}, y^{(2)}, \cdots, y^{(L)}\right] = \left[A^{(1)}w, A^{(2)}w, \cdots, A^{(L)}w\right], \tag{2}$$

where $A^{(l)}$ and $y^{(l)}$ are the sensing matrix and the measurement vector for l-th sampling, respectively. For the l-th sampling, the optimization is as follows:

$$P1 : \widehat{w} = \arg\min_{w} \left| y^{(l)} - A^{(l)}w \right|. \tag{3}$$

In practice, the target gestures are time-varying, requiring the relating sensing matrixes $A^{(l)}$. 1) when K target owns L different gestures, L^K different dictionaries are required to be built, which is a large amount of energy waste. 2) The target gestures change unpredictably and can not be detected before localization, making it impossible to choose the correct dictionary. 3) In most cases, we care more about the target locations but not the gestures. And the target gestures identification is much more difficult to be achieved. 4) The above issue is not the traditionally Multiple Measurement Vectors (MMV) [29] question, making it hard to find the proper result.

The target gestures may change, but the relationship among them always can be exploited. Following the idea in paper [30], we transfer the sensing matrixes $A^{(l)}$ to a fixed dictionary, and the optimal goal for the single sampling is as:

$$P2 : \widehat{w} = \arg\min_{w} \left| y^{(l)} - A\left(w - A^{-1}r^{(l)}\right) \right|, \tag{4}$$

where $r^{(l)}$ is a constant vector and A is the fixed sensing matrix. Then the location vector can be transferred as $w^{(l)} = w - A^{-1}r^{(l)}$. Compared with the original location vector w that is exactly sparse, the transferred one is an compressive one, in which only a few number of elements are large and the others are small enough to be neglected. Moreover, the index of the largest elements are the grid number of the target located at.

Then we transfer the above DFL issue as follows:

$$\left[y^{(1)}, y^{(2)}, \cdots, y^{(L)}\right] = A\left[w^{(1)}, w^{(2)}, \cdots, w^{(L)}\right], \tag{5}$$

where $y^{(l)}$ is the measurement vector based on the same target locations of the l-th sampling.

For above MMV recovery issue, we have transferred the relationship among different sensing matrixes into the correlation of the transferred location vectors. To improve the reconstruction accuracy, we exploit the block sparsity of the location vectors. As is shown in Figure 2, L location vectors are transferred as $\tilde{w}$ and then the localization equation can be represented as:

$$\tilde{y} = \tilde{A}\tilde{w} + \tilde{n}, \tag{6}$$

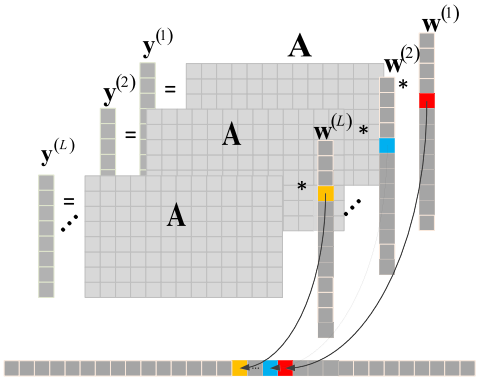

FIGURE 2. The illustration of DFL scheme with block sparsity.

where $\tilde{y}$, $\tilde{A}$, $\tilde{w}$ and $\tilde{n}$ are the vectored measurement vector, sensing matrix, Block sparsity vector and noise vector.

Block sparsity vector $\tilde{w}$: the vector is made up by L transferred location vectors $W = \left[w^{(1)}, w^{(2)}, \cdots, w^{(L)}\right]$ and:

$$\tilde{w} = vec\left(W^T\right), \tag{7}$$

where we can see that $\tilde{w}$ holds the block sparsity property of N blocks with a length of L. As the transferred location vectos, there is a correlation among i-th block $\tilde{w}_i = \left[w_i^{(1)}, w_i^{(2)}, \cdots, w_i^{(L)}\right]^T$ for they represent the same grid points. So this type of representation can well exploit the relationship of different location vectors.

Transferred sensing matrix $\tilde{A}$**:** the matrix can be represented as $\tilde{A} = A \otimes I_L$, where $\otimes$ is the Kronecker product and I_L is the unite matrix with the size of $L \times L$. Let $\tilde{A} = \left[\tilde{A}_1, \tilde{A}_2, \cdots, \tilde{A}_N\right]$, then the $n-th$ column is as follows:

$$\tilde{A}_n = \begin{bmatrix} A(:,n) & 0 & \cdots & 0 \\ 0 & A(:,n) & \cdots & 0 \\ \vdots & \vdots & \ddots & \vdots \\ 0 & 0 & \cdots & A(:,n) \end{bmatrix}_{ML \times L}, \quad n = (1, 2, \cdots, N) \tag{8}$$

where $A(:,n)$ is the n-th column of the matrix A. The transferred sensing matrix is only composed by the fixed dictionary, which is a replacement for the matrixes referring to different gestures.

transferred measurement vector $\tilde{y}$: contains all the measurement vectors received in L intervals and:

$$\tilde{y} = vec\left(\left[y^{(1)}, y^{(2)}, \cdots y^{(L)}\right]\right). \tag{9}$$

noise vector $\tilde{n}$**:** is utilized to approximate the noise and the most widely utilized one is the Gaussian white noise.

Above all, we research the different target motions and gestures in DFL, which can greatly approximate the real-world scene. Considering that the sensing matrixes for different gestures cannot be obtained, we apply the transferring method to builds the model only based on a fixed sensing matrix. And the issue is transferred as a block sparse vector recovery problem in order to exploit the correlation of the transferred location vectors.

IV. THE DETAILS OF THE GES-DFL RECOVERY ALGORITHM

In this section, we analyze the block sparsity and propose the novel Ges-DFL recovery algorithm to obtain the location vector.

A. THE FRAMEWORK OF VARIATIONAL EM ALGORITHM

The proposed Ges-DFL recovery algorithm is based on the variational Expect-Mean (EM) algorithm [31]. To better understand the framework of the variational EM algorithm, we firstly introduce the most popular Max-Likelihood (ML) estimation:

$$\tilde{\theta} = \arg\max_{\tilde{\theta}} \left(p\left(z;\theta\right)\right), \tag{10}$$

where z and θ are the observed variable and deterministic parameter, respectively, whose probabilistic relationship is described as $p(x;\theta)$. And for $p(x;\theta)$ here, θ is defined as random variable but not parameter. It is difficult or even impossible to compute $p(x;\theta)$ in practical scenes, thus the hidden variables x is introduced. Then, the log-likelihood function could be as:

$$\ln p\left(z;\theta\right) = \int q\left(x\right) \ln p\left(z;\theta\right) dx = F\left(q,\theta\right) + KL\left(q \,\|p\right) \tag{11}$$

in which:

$$F\left(q,\theta\right) = \int q\left(x\right) \ln\left(\frac{p\left(z,x;\theta\right)}{q\left(x\right)}\right) dx, \tag{12}$$

and

$$KL\left(q \,\|p\right) = -\int q\left(x\right) \ln\left(\frac{p\left(x|\, z;\theta\right)}{q\left(x\right)}\right) dx, \tag{13}$$

where $q(x)$ can be any probability density function. For $KL(q\,\|p)$, it is defined as the Kullback-Leibler divergence for $p(x|\, y;\theta)$ and $q(x)$. Finding that $KL(q\,\|p) \geq 0$, we can obtain the following inequation:

$$\ln p\left(z;\theta\right) \geq F\left(q,\theta\right), \tag{14}$$

which indicates that $F(q,\theta)$ is the lower bound of $\ln p(z;\theta)$ in case that $KL(q\,\|p) = 0$.

The EM algorithm can be obtained by the iteration of maximizing the lower bound $F(q,\theta)$ and the log-likelihood function:

$$\begin{aligned} &E-step: Evaluate \qquad p\left(x|\, z;\theta^{old}\right) \\ &M-step: Find \qquad \theta^{new} = \arg\max_{\theta} Q\left(\theta,\theta^{old}\right), \end{aligned} \tag{15}$$

where θ^{old} and θ^{new} are the current and the estimated parameters, respectively. And the lower bound $Q\left(\theta,\theta^{old}\right)$ can be obtained by substituting $q(x) = p\left(x|\, z;\theta^{old}\right)$ to Equation 13:

$$\begin{aligned} Q\left(\theta,\theta^{old}\right) &= \int p\left(x|\, z;\theta^{old}\right) \ln p\left(z,x;\theta\right) dx \\ &= \left\langle \ln p\left(y,x;\theta\right)\right\rangle_{p\left(x|z;\theta^{old}\right)}, \end{aligned} \tag{16}$$

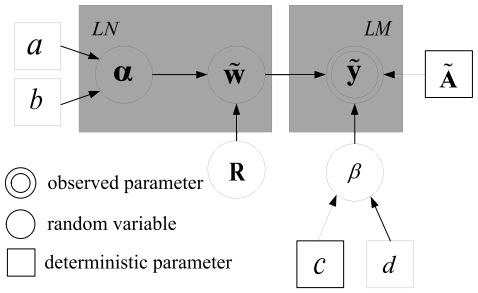

FIGURE 3. Graphical model of the Ges-DFL under variable Bayesian framework.

in which $\langle \ln p(z, x; \theta) \rangle_{p(x|z;\theta^{old})}$ presents the expectation of $\ln p(y, x; \theta)$ regarding to $p(x|y; \theta^{old})$. However, $p(x|z; \theta^{old})$ is too intractable to obtain in many interesting problems, which can be bypassed by providing an approximation for $q(x)$:

$$q(x) = \prod_i q_i(x_i) = \prod_i q_i, \tag{17}$$

where x is partitioned as different partitions x_i. Then the optimal posterior distribution in E-step can be calculated as:

$$\ln q_j = \langle \ln p(z, x; \theta) \rangle_{i \neq j}. \tag{18}$$

In summary, the posterior distribution and hidden variables could be updated iteratively through the E-step and the M-step. Based on the above EM framework, we will introduce our proposed Ges-DFL recovery algorithm in the following section.

B. THE GES-DFL RECOVERY ALGORITHM

To well analyse the Ges-DFL model, we illustrate variables of the DFL model in Figure 3. The transferred location vectors are all converted from the original location vector w, which composes of block sparse vectors $\tilde{w}$. Thus in order to exploit the block sparse of $\tilde{w}$, a two-layer hierarchical prior distribution is firstly imposed on w, which allows more flexibility when exploiting the characteristics compared with the stationary Gaussian distribution:

$$\begin{aligned} p(w|\alpha) &= \prod_{i=1}^{N} N\left(w_i|0, \alpha_i^{-1}\right) \\ &= \frac{1}{(2\pi)^{N/2}|B|^{-1/2}} \exp\left(-\frac{1}{2} w^T B w\right), \end{aligned} \tag{19}$$

where α_i is the inverse variance of w_i and $B = diag\left(\alpha_1^{-1}, \alpha_2^{-1}, \cdots, \alpha_N^{-1}\right)$ is the relating covariance matrix. And for $\alpha = [\alpha_1, \alpha_2 \cdots, \alpha_N]$, a Gamma prior distribution is imposed on it as follows:

$$\begin{aligned} p(\alpha; a, b) &= \prod_{i=1}^{N} Gamma(\alpha_i|a, b) \\ &= \prod_{i=1}^{N} \frac{1}{\int_0^\infty u^{a-1} e^{-u} du} b^a {\alpha_i}^{a-1} e^{-b\alpha_i}, \end{aligned} \tag{20}$$

in which a and b are the parameters set to constrain α, respectively.

As the i-th block of $\tilde{w}$, all elements within $\tilde{w}_i$ are transferred from w_i and share the similar localization information. Thus to exploit the relationship among them, R_i is introduced:

$$\begin{aligned} p(\tilde{w}_i; \alpha_i, R_i) &= N\left(\tilde{w}_i|0, {\alpha_i}^{-1} R_i\right) \\ &= \frac{1}{(2\pi)^{L/2}\left|{\alpha_i}^{-1} R_i\right|^{1/2}} \exp\left(-\frac{1}{2} \tilde{w}_i^T \alpha_i {R_i}^{-1} \tilde{w}_i\right), \end{aligned} \tag{21}$$

where R_i is set as a positive definite matrix to capture the correlation structure of $\tilde{w}_i$, which exploit the relationship among the i-th element of the different transferred vectors. Then, the posterior distribution for the block sparse vector $\tilde{w}$ can be calculated as:

$$p\left(\tilde{w}; \{\alpha_i, R_i\}_1^N\right) = N\left(\tilde{w}|0, \tilde{\Sigma}\right), \tag{22}$$

with $\tilde{\Sigma}$ as its covariance matrix:

$$\tilde{\Sigma} = \begin{bmatrix} {\alpha_1}^{-1} R_1 & 0 & \cdots & 0 \\ 0 & {\alpha_2}^{-1} R_2 & \cdots & 0 \\ \vdots & \vdots & \ddots & \vdots \\ 0 & 0 & \cdots & {\alpha_N}^{-1} R_N \end{bmatrix}. \tag{23}$$

For the noise vector $\tilde{n}$, the posterior distribution is particularly imposed as follows:

$$p(\tilde{n}|\beta) = N(\tilde{n}|0, \beta I), \tag{24}$$

in which β is the variance and I is the unite matrix with size $LM \times LM$, respectively. In order to better approximate the varying environment, the parameter β in the noise model is assumed to be the Gamma distribution with the parameters c and d:

$$\begin{aligned} p(\beta; c, d) &= Gamma(\beta|c, d) \\ &= \frac{1}{\int_0^\infty u^{c-1} e^{-u} du} b^c {\alpha_i}^{c-1} e^{-d\beta}., \end{aligned} \tag{25}$$

Then we can obtain the following likelihood function regarding to the transferred sensing equation:

$$p(\tilde{y}|\tilde{w}, \beta) = \left(2\pi\beta^{-1}\right)^{-ML/2} \exp\left(-\frac{\beta}{2} \left\|\tilde{y} - \tilde{A}\tilde{w}\right\|_2^2\right) \tag{26}$$

Under the Bayesian framework, the distribution of $p(\tilde{w}, \alpha, \beta|\tilde{y})$ should be calculated:

$$p(\tilde{w}, \alpha, \beta|\tilde{y}) = \frac{p(\tilde{y}|\tilde{w}, \beta)\, p\left(\tilde{w}; \{\alpha_i, B_i\}_{i=1}^N\right) p(\alpha)\, p(\beta)}{p(\tilde{y})} \tag{27}$$

in which the probability distribution in the numerator can be calculated according to the Ges-DFL model. And for $p(\tilde{y})$ in the numerator, it is as:

$$p(\tilde{y}) = \int p(\tilde{y}|\tilde{w}, \beta)\, p\left(\tilde{w}; \{\alpha_i, R_i\}_{i=1}^N\right) p(\alpha)\, p(\beta)\, d\tilde{w} d\alpha d\beta, \tag{28}$$

which could not be analytically calculated, thus variational inference is required. According to above analyse, the block sparse vector $\tilde{w}$ and the noise vector $\tilde{n}$, including the depending parameters shown in Figure3, are all obviously independent. Then Equation(27) can be calculated as:

$$p(\tilde{w}, \alpha, \beta | \tilde{y}; a, b, c, d) \approx q(\tilde{w}, \alpha, \beta) = q(\tilde{w}) q(\alpha) q(\beta). \tag{29}$$

Considering that the block sparse vector $\tilde{w}$ is determined not only by α but also the correlation matrix R_i $(i = 1, 2, \cdots, N)$, two steps are required to compute the posterior: the designing of the relation matrix $\{R_i\}_{i=1}^N$ and the updating of the variables $\tilde{w}$, α and β.

Updating of $\tilde{w}$

$$\begin{aligned}
&\ln q(\tilde{w}) \\
&= \langle \ln p(\tilde{w}, \alpha, \beta) \rangle_{q(\alpha)q(\beta)} + C \\
&= \left\langle \ln p(\tilde{y} | \tilde{w}, \beta) p\left(\tilde{w}_i; \{\alpha_i, R_i\}_1^N\right) \right\rangle_{q(\alpha)q(\beta)} + C \\
&= \left\langle -\frac{\beta}{2}\left(\tilde{y} - \tilde{A}\tilde{w}\right)^T \left(\tilde{y} - \tilde{A}\tilde{w}\right) - \frac{1}{2}\tilde{w}^T \Sigma^{-1} \tilde{w} \right\rangle_{q(\alpha)q(\beta)} + C \\
&= -\frac{\langle\beta\rangle}{2}\left(\tilde{w}^T \tilde{A}^T \tilde{A}\tilde{w} - 2\tilde{w}^T \tilde{A}^T \tilde{y}\right) - \frac{1}{2}\tilde{w}^T \left\langle \Sigma^{-1} \right\rangle \tilde{w} + C \\
&= -\frac{1}{2}\tilde{w}^T \left(\langle\beta\rangle \tilde{A}^T \tilde{A} + \Sigma^{-1}\right) \tilde{w} + \langle\beta\rangle \tilde{w}^T \tilde{A}^T \tilde{y} + C,
\end{aligned} \tag{30}$$

where we can see that the block sparse vector holds the Gaussian posterior distribution:

$$q(\tilde{w}) = N(\tilde{w} | \mu, \Sigma), \tag{31}$$

with

$$\mu = \langle\beta\rangle \Sigma \tilde{w}^T \tilde{A}^T \tag{32}$$

$$\Sigma = \left(\langle\beta\rangle \tilde{A}^T \tilde{A} + \tilde{\Sigma}^{-1}\right)^{-1}. \tag{33}$$

in which the inverse operation in Equation(33) is always complicated. To reduce the high calculate complexity, we calculate the covariance matrix Σ as follows:

$$\Sigma = \tilde{\Sigma}^{-1} - \tilde{\Sigma}^{-1} \tilde{A}^T E^{-1} \tilde{A} \tilde{\Sigma}^{-1}, \tag{34}$$

with

$$E = \langle\beta\rangle^{-1} I + \tilde{A}\tilde{\Sigma}^{-1}\tilde{A}^T. \tag{35}$$

in which $\tilde{\Sigma}$ is a block diagonal matrix, whose inverse matrix is easy to calculate. In addition, E owns lower dimensions of $LM \times LM$ when compared with $\langle\beta\rangle \tilde{A}^T \tilde{A} + \Sigma^{-1}$ of $LN \times LN$, thus the operation in Equation(34) can reduce the compute complexity form $O\left(L^3 M^3\right)$ in to $O\left(L^3 M^3\right)$

Updating of α

$$\begin{aligned}
\ln q(\alpha) &= \langle \ln p(\tilde{w}, \alpha, \beta) \rangle_{q(\alpha)q(\tilde{w})} + C \\
&= \left\langle \ln p\left(\tilde{w}; \{\alpha_i, R_i\}_1^N\right) p(\alpha) \right\rangle_{q(\tilde{w})} + C \\
&= \left\langle \begin{array}{l} -\frac{1}{2}\ln\left|\tilde{\Sigma}\right| - \frac{1}{2}\tilde{w}^T \tilde{\Sigma}^{-1} \tilde{w} \\ +(a-1)\sum_i \ln a_i - b\sum_i a_i \end{array} \right\rangle_{q(\tilde{w})} + C \\
&= \frac{L}{2}\sum_i \ln a_i - \frac{1}{2}\sum_i a_i \left(tr\left(\Sigma_i + \mu_i \mu_i^T\right)\right) \\
&\quad + (a-1)\sum_i \ln a_i - b\sum_i a_i + C \\
&= \left(a + \frac{L}{2} - 1\right)\sum_i \ln a_i \\
&\quad - \sum_i \left(b + \frac{1}{2} tr\left(\Sigma_i + \mu_i \mu_i^T\right)\right) a_i + C,
\end{aligned} \tag{36}$$

which obviously shows that the posterior distribution of the variable α is as:

$$p\left(\alpha; \tilde{a}, \tilde{b}\right) = \prod_{i=1}^N Gamma\left(\alpha_i | \tilde{a}, \tilde{b}\right), \tag{37}$$

with

$$\tilde{a} = a + \frac{L}{2}. \tag{38}$$

$$\tilde{b}_m = b + \frac{1}{2} tr\left(R_i^{-1}\left(\Sigma_i + \mu_i \mu_i^T\right)\right). \tag{39}$$

in which $tr(\cdot)$ represents the trace of the matrix. $\mu_i \in R^{L\times 1}$ and $\Sigma_i \in R^{L\times L}$ are means and covariance of the i-th block of $\tilde{w}_i \in R^{L\times 1}$, respectively.

Updating of β

$$\begin{aligned}
\ln q(\beta) &= \langle \ln p(\tilde{w}, \alpha, \beta) \rangle_{q(\alpha)q(\tilde{w})} + C \\
&= \langle \ln p(\tilde{y} | \tilde{w}, \beta) p(\beta) \rangle_{q(\alpha)q(\tilde{w})} + C \\
&= \frac{ML}{2}\ln\beta - \left\langle \frac{\beta}{2}\left(\tilde{y} - \tilde{A}\tilde{w}\right)^T \left(\tilde{y} - \tilde{A}\tilde{w}\right) \right\rangle \\
&\quad + (c-1)\ln\beta - d\beta + C \\
&= \left(c + \frac{ML}{2} - 1\right)\ln\beta \\
&\quad - \left(\begin{array}{l} d + \frac{1}{2}\left(\left\|\tilde{y} - \tilde{A}\mu\right\|_2^2\right) \\ +tr\left(\tilde{A}\Sigma\tilde{A}^T\right) \end{array} \right)\beta + C \\
&= \left(\hat{c} - 1\right) ln\beta - \hat{d}\beta + C,
\end{aligned} \tag{40}$$

where the posterior distribution of β follows Gamma distribution with the parameters:

$$\hat{c} = c + \frac{ML}{2}. \tag{41}$$

$$\hat{d} = d + \frac{1}{2}\left(\left\|\tilde{y} - \tilde{A}\mu\right\|_2^2\right) + tr\left(\tilde{A}\Sigma\tilde{A}^T\right). \tag{42}$$

Updating of R_i

As stated above, R_i is the correlation matrix of the i-th block of $\tilde{w}$, represented as $\tilde{w}_i$. The above variables are based on an accurate estimation of R_i. Under the EM framework, R_i is set as a variable to be estimated in M-step. According to Equation 23, N matrixes $\{R_i\}_{i=1}^N$ are required to describe the different correlations for N blocks, whose number is not as much as the measurements and may causing overfitting issues. Coming to this, the same correlation matrix R are assumed to all the blocks. Moreover, the target always

changes unpredictably in practice, making it unreasonable to restrain the correlation matrix R before. Thus no prior structure is imposed on the correlation matrix R to better approximate the real-world scene.

According to the definition of function $Q(\cdot)$ in Equation 16, R is updated as follows:

$$\begin{aligned}\tilde{R} &= \arg\max_{R} Q\left(R, R^{old}\right) \\ &= \arg\max_{R} \langle \ln p\left(\tilde{y}, \tilde{w}, \alpha, \beta; R\right)\rangle_{q(\alpha)q(\tilde{w})q(\beta)} \\ &= \arg\max_{R} \langle \ln p\left(\tilde{w}|\,\alpha; R\right)\rangle_{q(\alpha)}, \end{aligned} \tag{43}$$

where R^{old} and $\tilde{R}$ are the current and the estimated correlation matrix for R, respectively. $q(\tilde{w})$, $q(\alpha)$ and $q(\beta)$ are the posterior distributions with respect to the current correlation matrix R. According to Equation 21, we can obtain that $p\left(\tilde{w}|\,\alpha; R\right) = N\left(0, B^{-1} \otimes R\right)$. Thus, the above optimal issue can be represented as:

$$\begin{aligned}\tilde{R} &= \arg\min_{R} \left\{ N \ln |R| + \left\langle \tilde{w}^T \left(B^{-1} \otimes R\right) \tilde{w} \right\rangle_{q(\alpha)} \right\} \\ &= \arg\min_{R} \left\{ N \ln |R| + tr\left[\left(B^{-1} \otimes R\right) \tilde{\Sigma} + \tilde{\mu}\tilde{\mu}^T \right] \right\}. \end{aligned} \tag{44}$$

To find the minimal result of the above optimal issue, set

$$f(R) = N \ln |R| + tr\left[\left(B^{-1} \otimes R\right) \tilde{\Sigma} + \tilde{\mu}\tilde{\mu}^T \right], \tag{45}$$

where $f(R)$ is the function of R with the other variables settled. Then its gradient is computed as:

$$\frac{\partial f(R)}{\partial R} = NR^{-1} - \sum_{i=1}^{N} \alpha_i R^{-1} \left(\tilde{\Sigma}_i + \tilde{\mu}_i \tilde{\mu}_i^T\right) R^{-1}. \tag{46}$$

According to the property of gradient, we set the $\frac{\partial f(R)}{\partial R} = 0$, then the optimal result of $f(R)$ can be updated as:

$$R = \frac{1}{N} \sum_{i=1}^{N} \alpha_i \left(\tilde{\Sigma}_i + \tilde{\mu}_i \tilde{\mu}_i^T\right), \tag{47}$$

where $\mathbf{R}$ is the optimal result to approximate the relationship among all the transferred location vectors.

In summary, Ges-DFL scheme is built as a block compressive sensing recovery issue in the previous section and then solved under the variational EM framework. In the E-step, the variables including $\tilde{w}$, α and β are all imposed the flexible posterior distributions with respect to R, and then their determining parameters are estimated by variational Bayesian inference. In the M-step, the correlation matrix R based on the other variables is learned by its gradient. Thus, by operating the two steps iteratively, $\tilde{w}$ will be achieved. The estimated location vector can be estimated as:

$$w_i = \frac{1}{L} \sum_{l=1}^{L} \tilde{w}_i^l, \tag{48}$$

where $\tilde{w}_i^l$ is the l-th element in the $i-th$ block sparse of $\tilde{w}$.

Now, we summarize the Ges-DFL algorithm in details as algorithm 1.

Algorithm 1 The Algorithm of Ges-DFL

Require: $\tilde{y}, \tilde{A}, \tau_{\max}, \delta$.
Ensure:
Initialize the parameters $a = b = c = d = 10^{-6}$.
Initialize the correlation matrix $R = I_L$.
Initialize $\alpha^{(0)}$, $\tilde{w}^{(0)}$ and $\beta^{(0)}$ according to (20), (21) and (25).
Set the iteration number $\tau = 1$.
while $\tau < \tau_{\max}$ and $\Delta r > \delta$ **do**
  Update posterior distribution of $\alpha^{(\tau)}$ using (37)-(39).
  Update posterior distribution of $\beta^{(\tau)}$ using (40)-(42).
  Update posterior distribution of $\tilde{w}^{(\tau)}$ using (31)-(35).
  Update correlation matrix R using (47).
  Compute the reduction using $\Delta\tau = \left\|\alpha^{(\tau)} - \alpha^{(\tau-1)}\right\|_2 / \left\|\alpha^{(\tau)}\right\|_2$;
  $\tau = \tau + 1$.
end while
Estimate the current distribution mean μ and $\tilde{w}$.
Output the the estimation of the location vector using 48).

An uninformative distribution is assumed on the variables in order to achieve better results, thus the parameters are set as $a = b = c = d = 10^{-6}$ as is shown in the algorithm. $\Delta\tau$ is the reduction of the current and the estimated α utilized to balance the convergence. The iteration will be terminated when the maximum iteration number $\tau_{\max}$ is reached or the reduction threshold δ is reached. The correlation matrix R describes the relationship of different gestures, which is impossible for us to determine. Thus to initialize, $R = I_L$ is settled in the first iteration.

V. SIMULATIONS

We investigate the DFL issue for multiple targets with different gestures in this paper and propose a new algorithm based on variational Bayesian inference called Ges-DFL. To testify the localization performance, we formulate the following simulations.

A. THE SIMULATION PERFORMANCE

We perform the simulation in the detecting area with the length of $20m \times 20m$, which is divided into $N = 100$ grids and $M = 20$ wireless links are applied to measure the RSS changes. In addition, the Gaussian white noise is added to approximate the noise, represented as Signal-to-Noise Ratio (SNR). According to the transferring method, the location vector in the l-th time interval is approximated as follows to represent the influence of the location vectors [29]:

$$w^{(l)} = w^{(0)} - A^{-1} r^{(l)}, \tag{49}$$

where $w^{(0)}$ and $w^{(l)}$ are the real location vector and the transferred location vector of l-th time interval, respectively. Thus the RSS changes caused by different targets can be modeled as $y^{(l)} = Aw^{(l)} + n^{(l)}$. The changing parameters $r^{(l)}$ is utilized

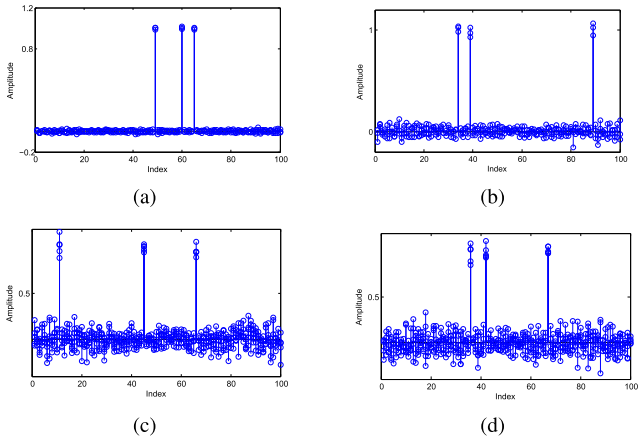

FIGURE 4. The transferred location vectors under different changing parameter. (a) $\mu_r = 0, \sigma_r = 0.1$; (b)$\mu_r = 0, \sigma_r = 0.5$; (c) $\mu_r = 0, \sigma_r = 2$; (d) $\mu_r = 1, \sigma_r = 2$.

to induce the changes caused by different target gestures, on which a Gaussian noise is imposed $r^{(l)} = N\left(r^{(l)} \middle| \mu_r, \sigma_r\right)$.

To measure the algorithm performance, the average localization error $AvgE$ is introduced:

$$AvgE = \sum_{i=1}^{S}\sum_{k=1}^{K}\frac{1}{K \cdot S}\sqrt{\left(x_k^i - \hat{x}_k^i\right)^2 + \left(y_k^i - \hat{y}_k^i\right)^2}, \quad (50)$$

where $\left(x_k^i, y_k^i\right)$ and $\left(\hat{x}_k^i, \hat{y}_k^i\right)$ are the real target location and the estimated target location for the k-th target in i-th simulation, respectively. K and S are the target numer and the simulation number.

Also, the state-of-art recovery algorithm is applied to compare with the Ges-DFL algorithm, including Temporally Sparse Bayesian Learning (TSBL) [32], Multiple-Focal Underdetermined System Solver (M-FOCUSS) [33], Multiple Greedy Marching Pursuit (MGMP) [34], Simultaneous Orthogonal Marching Pursuit SOMP [35] and Variational Bayesian Expect-Mean (VBEM) [31].

B. THE ANALYSING OF GES-DFL RECOVERY ALGORITHM

Firstly, we analyse the changing parameters applied to approximate the different target gestures. Figure4 illustrates the transferred location vectors under different changing parameters. All the transferred location vectors are compressive but not precisely sparse, and they vary with the values of μ_r and σ_r. The different values are applied to approximate the different gestures of the target. The larger the values are, the less sparse of the transferred location vectors.

Secondly, the recovered location vectors are analysed. The target may be with different gestures, leading to the transferred location vector $w^{(l)}$ not exactly sparse under the fixed sensing matrix. And among different sampling intervals, the transferred vector is different. However, as stated above, different transferred vectors represent the same target location, where the most significant elements of the location vectors represents the same location. In Figure 5, we can see that the proposed algorithm can recover the location vector even when the transferred location vectors are not

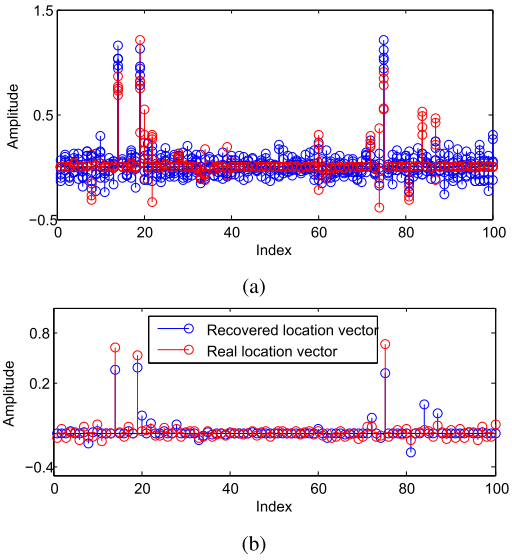

FIGURE 5. The illustration of the recovered location vectors and the real target location. (a) The L transferred location vectors; (b) The average of L transferred location vectors;.

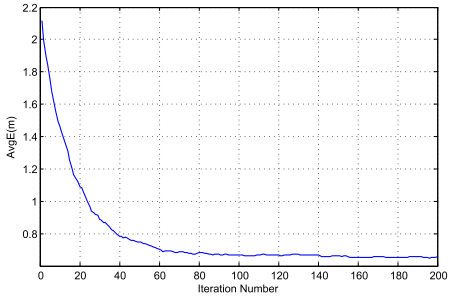

FIGURE 6. The localization error via different iteration numbers.

exactly sparse. In Figure 5(a), it is obvious that the recovered block sparse vectors under the same sensing matrix is not similar to the original vector. However, as is shown in Figure 5(b), the recovered location vector, which is the average of all the estimated L transferred location vectors, can represent the target location well.

Thirdly, we test the localization performance via different iteration numbers of the Ges-DFL. The samplings with $L = 5$ time intervals for $K = 3$ targets and $N = 100$ grids are collected to localize. Also, the changing parameters are set as $r = N(r|0, 0.5)$ and the Signal to Noise Ratio (SNR) is $30dB$. As is shown in Figure 6, with the increasing of the iteration number, the localization error reduces quickly. Moreover, the $AvgE$ value becomes convergence when the iteration number reaches to 180. Thus the maximum iteration number is settled as 200 to both ensure the localization accuracy and the effectiveness.

C. THE PERFORMANCE VIA OTHER ALGORITHMS

Firstly, we test the localization performance via different time intervals. More samplings can provide more localization information, surely guaranteeing a more accurate localization result. As is shown in Figure 7, with the increasing of the

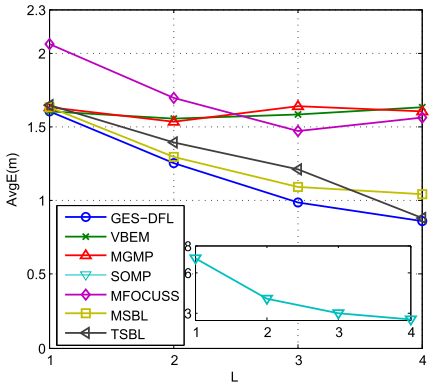

FIGURE 7. The localization performance via different time intervals.

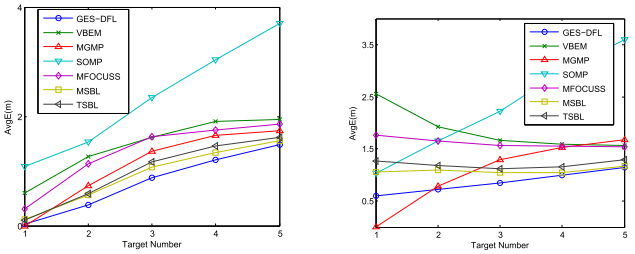

FIGURE 8. The localization performance via different target number. **(a)** $\mu_r = 0$, $\sigma_r = 0.1$; **(b)** $\mu_r = 0$, $\sigma_r = 0.5$.

samplings number L, the localization error decreased for all the algorithms.And the proposed Ges-DFL localization can achieve the lowest localization error when compared with others. Although more samplings will promise more accurate localization, it can also influence the synchronization. Thus we choose $L = 3$ in the following simulations.

Then the algorithm performance is tested through different target number. As we can see from Figure 8, the localization accuracy becomes lower with the increasing of the target number for all the algorithms. The target number indicates the sparse property of the location vector. Larger the target number is, lower sparsity of the location vector owns, undoubtedly influencing the recovery accuracy. In Figure 8(a), the Ges-DFL owns the lowest localization error among all the algorithms.And the localization error is higher for the proposed Ges-DFL compared with MGMP in Figure 8(b) when $k = 1$, because the transferred location vectors are too compressive. And when the target number reaches to 2, the proposed Ges-DFL performs better than other algorithms.

Finally, we test the algorithm via different noise with the SNR varies from $5dB$ to $65dB$. When $k = 3$, the localization error of different algorithms via the SNR is shown in Figure 9(a). The localization error decreased for all the algorithms with the increasing of the SNR. We notice that when $SNR = 5dB$, the $AvgE$ for the MGMP is lower than the Ges-DFL, which can not prove that the MGMP performs out the Ges-DFL. In fact, when $SNR = 5dB$, the localization error is too large to serve a reliable result for all the algorithms. When the SNR is increasing, for the proposed algorithm Ges-DFL,

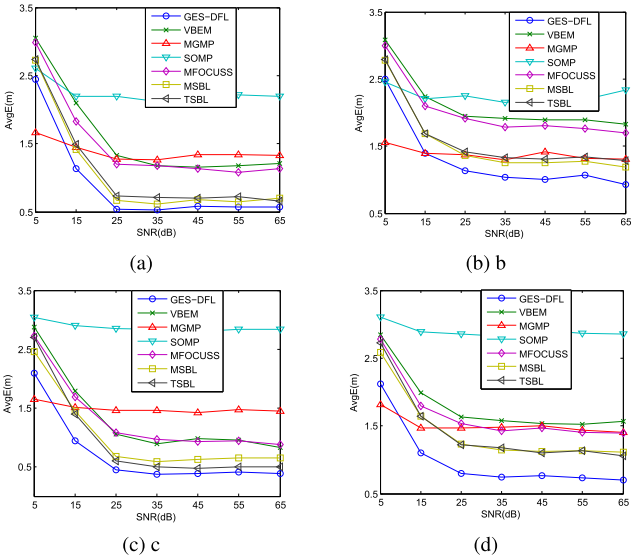

FIGURE 9. The localization performance via different target number. **(a)** $M = 20, K = 3, \sigma_r = 0.5$; **(b)** $M = 20, K = 3, \sigma_r = 0.8$; **(c)** $M = 26, K = 4, \sigma_r = 0.5$; **(d)** $M = 26, K = 4, \sigma_r = 0.8$.

it performs the best. The same conclusion can be obtained from Figure 9 (b), (c) and (d).

VI. CONCLUSION

We propose a new localization algorithm Ges-DFL in this paper, which considers the different target gestures in DFL scheme. Firstly, recognizing that dictionaries referring to different target gestures can not be obtained, we transfer the relationship of dictionaries to the correlation of the location vectors, where only a fixed dictionary is needed. Secondly, the location vectors are transferred under the same sensing matrix, and the DFL scheme is built as an MMV recovery issue. Thirdly, we exploit the block sparsity of the transferred location vectors and propose a new algorithm named Ges-DFL using the variational Bayesian inference. Finally, simulations show the accuracy and robustness of the Ges-DFL algorithm.

REFERENCES

[1] H. Suo, J. Wan, L. Huang, and C. Zou, "Issues and challenges of wireless sensor networks localization in emerging applications," in *Proc. Int. Conf. Comput. Sci. Electron. Eng.*, Mar. 2012, pp. 447–451.

[2] I. F. Akyildiz, W. Su, Y. Sankarasubramaniam, and E. Cayirci, "Wireless sensor networks: A survey," *Comput. Netw.*, vol. 38, no. 4, pp. 393–422, Mar. 2002.

[3] A. Awad, T. Frunzke, and F. Dressler, "Adaptive distance estimation and localization in WSN using RSSI measures," in *Proc. 10th Euromicro Conf. Digit. Syst. Design Archit., Methods Tools (DSD)*, Aug. 2007, pp. 471–478.

[4] N. Patwari and J. Wilson, "RF sensor networks for device-free localization: Measurements, models, and algorithms," *Proc. IEEE*, vol. 98, no. 11, pp. 1961–1973, Nov. 2010.

[5] F. Adib, H. Mao, Z. Kabelac, D. Katabi, and R. C. Miller, "Smart homes that monitor breathing and heart rate," in *Proc. 33rd Annu. ACM Conf. Hum. Factors Comput. Syst. (CHI)*, Apr. 2015, pp. 837–846.

[6] A. Ledeczi, P. Valgyesi, M. Maroti, G. Simon, G. Balogh, A. Nadas, B. Kusy, S. Dora, and G. Pap, "Multiple simultaneous acoustic source localization in urban terrain," in *Proc. 4th Int. Symp. Inf. Process. Sensor Netw. (IPSN)*, Apr. 2005, pp. 24–27.

[7] J. Han, C. Qian, X. Wang, D. Ma, J. Zhao, W. Xi, Z. Jiang, and Z. Wang, "Twins: Device-free object tracking using passive tags," *IEEE/ACM Trans. Netw.*, vol. 24, no. 3, pp. 1605–1617, Jun. 2016.
[8] M. Moussa and M. Youssef, "Smart cevices for smart environments: Device-free passive detection in real environments," in *Proc. IEEE Int. Conf. Pervas. Comput. Commun.*, Mar. 2009, pp. 1–6.
[9] M. Youssef, M. Mah, and A. Agrawala, "Challenges: Device-free passive localization for wireless environments," in *Proc. 13th Annu. ACM Int. Conf. Mobile Comput. Netw. (MobiCom)*, Sep.2007, pp. 222–229.
[10] C. Xu, B. Firner, R. S. Moore, Y. Zhang, W. Trappe, R. Howard, F. Zhang, and N. An, "SCPL: Indoor device-free multi-subject counting and localization using radio signal strength," in *Proc. 12th Int. Conf. Inf. Process. Sensor Netw. (IPSN)*, Apr. 2013, pp. 8–11.
[11] P. Wu, X. Wu, G. Chen, M. Shan, and X. Zhu, "A few bits are enough: Energy efficient device-free localization," *Comput. Commun.*, vol. 83, pp. 72–80, Jun. 2016.
[12] E. J. Candes and M. B. Wakin, "An introduction to compressive sampling," *IEEE Signal Process. Mag.*, vol. 25, no. 2, pp. 21–30, Mar. 2008.
[13] J. Wang, D. Fang, X. Chen, Z. Yang, T. Xing, and L. Cai, "LCS: Compressive sensing based device-free localization for multiple targets in sensor networks," in *Proc. IEEE INFOCOM*, Apr. 2013, pp. 145–149.
[14] D. Yu, Y. Guo, N. Li, and D. Fang, "Dictionary refinement for compressive sensing based device-free localization via the variational EM algorithm," *IEEE Access*, vol. 4, pp. 9743–9757, 2016.
[15] L. Chang, X. Chen, D. Fang, J. Wang, and Z. Tang, "FALE: Fine-grained device free localization that can adaptively work in different areas with little effort," *ACM SIGCOMM Comput. Commun. Rev.*, vol. 45, no. 5, pp. 601–602, Aug. 2015.
[16] Y. Wang, K. Wu, and L. M. Ni, "WiFall: Device-free fall detection by wireless networks," *IEEE Trans. Mobile Comput.*, vol. 16, no. 2, pp. 581–594, Feb. 2017.
[17] Y. Wang, J. Liu, Y. Chen, M. Gruteser, J. Yang, and H. Liu, "E-eyes: Device-free location-oriented activity identification using fine-grained WiFi signatures," in *Proc. 20th Annu. Int. Conf. Mobile Comput. Netw. (MobiCom)*, Sep. 2014, pp. 617–628.
[18] J. Wang, X. Zhang, Q. Gao, H. Yue, and H. Wang, "Device-free wireless localization and activity recognition: A deep learning approach," *IEEE Trans. Veh. Technol.*, vol. 66, no. 7, pp. 6258–6267, Jul. 2017.
[19] J. Wang, Q. Gao, H. Wang, and X. Zhang, "Device-free localisation with wireless networks based on compressive sensing," *IET Commun.*, vol. 6, no. 15, pp. 2395–2403, Oct. 2012.
[20] D. Bolme, J. R. Beveridge, B. A. Draper, and Y. M. Lui, "Visual object tracking using adaptive correlation filters," in *Proc. IEEE Comput. Soc. Conf. Comput. Vis. Pattern Recognit.*, Jun. 2010, pp. 2544–2550.
[21] X. Jia, H. Lu, and M.-H. Yang, "Visual tracking via adaptive structural local sparse appearance model," in *Proc. IEEE Conf. Comput. Vis. Pattern Recognit.*, Jun. 2012, pp. 1822–1829.
[22] D. Hauschildt and N. Kirchhof, "Advances in thermal infrared localization: Challenges and solutions," in *Proc. Int. Conf. Indoor Positioning Indoor Navigat.*, Sep. 2010, pp. 1–8.
[23] J. Xiao, K. Wu, Y. Yi, L. Wang, and L. M. Ni, "Pilot: Passive device-free indoor localization using channel state information," in *Proc. IEEE 33rd Int. Conf. Distrib. Comput. Syst.*, Jul. 2013, pp. 236–245.
[24] M. Seifeldin, A. Saeed, A. E. Kosba, A. El-Keyi, and M. Youssef, "Nuzzer: A large-scale device-free passive localization system for wireless environments," *IEEE Trans. Mobile Comput.*, vol. 12, no. 7, pp. 1321–1334, Jul. 2013.
[25] D. Zhang, K. Lu, R. Mao, Y. Feng, Y. Liu, Z. Ming, and L. M. Ni, "Fine-grained localization for multiple transceiver-free objects by using RF-based technologies," *IEEE Trans. Parallel Distrib. Syst.*, vol. 25, no. 6, pp. 1464–1475, Jun. 2014.
[26] Y. Zhao and N. Patwari, "Robust estimators for variance-based device-free localization and tracking," *IEEE Trans. Mobile Comput.*, vol. 14, no. 10, pp. 2116–2129, Oct. 2015.
[27] J. Wang, Q. Gao, M. Pan, X. Zhang, Y. Yu, and H. Wang, "Toward accurate device-free wireless localization with a saddle surface model," *IEEE Trans. Veh. Technol.*, vol. 65, no. 8, pp. 6665–6677, Aug. 2016.
[28] J. Wang, D. Fang, Z. Yang, H. Jiang, X. Chen, T. Xing, and L. Cai, "E-HIPA: An energy-efficient framework for high-precision multi-target-adaptive device-free localization," *IEEE Trans. Mobile Comput.*, vol. 16, no. 3, pp. 716–729, Mar. 2017.
[29] S. F. Cotter, B. D. Rao, K. Engan, and K. Kreutz-Delgado, "Sparse solutions to linear inverse problems with multiple measurement vectors," *IEEE Trans. Signal Process.*, vol. 53, no. 7, pp. 2477–2488, Jul. 2005.
[30] J. Wang, X. Chen, D. Fang, C. Q. Wu, Z. Yang, and T. Xing, "Transferring compressive-sensing-based device-free localization across target diversity," *IEEE Trans. Ind. Electron.*, vol. 62, no. 4, pp. 2397–2409, Apr. 2015.
[31] D. G. Tzikas, A. C. Likas, and N. P. Galatsanos, "The variational approximation for Bayesian inference life after the em algorithm," *IEEE Signal Process. Mag.*, vol. 25, no. 6, pp. 131–146, Nov. 2008.
[32] Z. Zhang and B. D. Rao, "Extension of SBL algorithms for the recovery of block sparse signals with intra-block correlation," *IEEE Trans. Signal Process.*, vol. 61, no. 8, pp. 2009–2015, Apr. 2013.
[33] R. Zdunek and A. Cichocki, "Improved M-FOCUSS algorithm with overlapping blocks for locally smooth sparse signals," *IEEE Trans. Signal Process.*, vol. 56, no. 10, pp. 4752–4761, Oct. 2008.
[34] E. Lagunas, S. K. Sharma, S. Chatzinotas, and B. Ottersten, "Compressive sensing based target counting and localization exploiting joint sparsity," in *Proc. IEEE Int. Conf. Acoust., Speech Signal Process. (ICASSP)*, Mar. 2016, pp. 20–25.
[35] J.-F. Determe, J. Louveaux, L. Jacques, and F. Horlin, "On the noise robustness of simultaneous orthogonal matching pursuit," *IEEE Trans. Signal Process.*, vol. 65, no. 4, pp. 864–875, Feb. 2017.

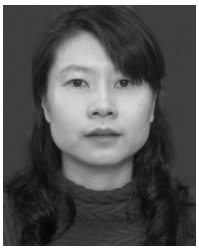

YAN GUO received the B.S. and M.S. degrees from the PLA Institute of Information Engineering, Zhengzhou, China, in 1993 and 1996, respectively, and the Ph.D. degree from Xidian University, Xi'an, China, in 2002. She has been a Visiting Scholar with Chonbuk National University, South Korea. She is currently a Professor with the College of Communications Engineering, Army Engineering University, Nanjing, China. Her main research interests include the Internet of Things, compressed sensing, and big data.

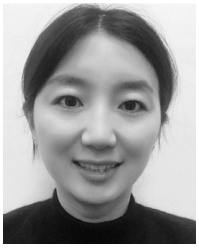

SIXING YANG received the M.S. degree from the Army Engineering University of PLA, Nanjing, China, in 2017, where she is currently pursuing the Ph.D. degree with the College of Communication Engineering. Her current research interests include the Internet of Things, wireless networks, and device-free target localization.

NING LI received the B.S. and M.S. degrees from the PLA Institute of Information Engineering, Zhengzhou, China, in 1989 and 1996, respectively. He is currently an Associate Professor with the College of Communications Engineering, Army Engineering University, Nanjing, China. His main research interests include Ad hoc networks, digital beamforming, and machine learning.

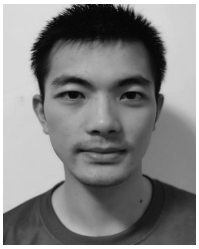

XINHUA JIANG received the B.E. degree from Army Engineering University, China, in 2018, where he is currently pursuing the M.E. degree. His research interests include device free wireless localization and information processing.